# Richter's laws at the laboratory scale interpreted by acoustic emission

A. Carpinteri*, G. Lacidogna* and N. Pugno*

*Politecnico di Torino*

*In the present work the acoustic emission (AE) technique is applied to examine some aspects influencing concrete failure in compression. By monitoring a structure by means of the AE technique, it proves possible to detect the occurrence of stress-induced cracks. Cracking, in fact, is accompanied by the emission of elastic waves that propagate within the bulk of the material. These waves can be received and recorded by transducers applied to the surface of the structural elements. This technique can be used for diagnosing structural damage phenomena. The current paper presents a mixed experimental and theoretical approach to evaluate the energy density dissipated during compression at each value of strain. Through this method, the two semi-empirical Gutenberg–Richter (GR) laws, well-known in seismology, are verified, the fractal interpretation results of which are very close to the essence of the AE phenomenon. Furthermore, the mentioned approach allows the parameter of 'magnitude' to be identified, appearing in the laws, with the number of oscillations larger than a given threshold measured in volts. Finally, the developed concepts are applied to the study of the compression phenomenon. In particular, by this approach, it is possible to distinguish between the energy progressively dissipated or stored in a compressed structural element.*

## Notation

| | |
|---|---|
| $a, b, C, \bar{C}$ | Gutenberg–Richter (GR) law experimental coefficients |
| $\bar{\bar{C}}, c$ | cumulative distribution law coefficients |
| $D$ | fractal exponent |
| $d$ | specimen diameter |
| $E$ | energy released during an event of intensity $m$ |
| $E_{\min}$ | minimum detectable released energy |
| $h$ | specimen height |
| $I$ | number of steps |
| $I_{\text{TOT}}$ | total number of steps |
| $k$ | stiffness |
| $m$ | GR law earthquake magnitude |
| $\bar{m}$ | mass |
| $N$ | number of AE oscillations in a time interval $\Delta t$ |
| $N_c$ | cumulative number of AE oscillations |
| $N(v)$ | cumulative distribution of AE signals |
| $n$ | number of events larger than $m$, or number of particles with radius larger than $r$ |
| $n_{\text{tot}}$ | total number of events, or total number of particles |
| $M(< r)$ | mass of fragments with radius smaller than $r$ |
| $M$ | total mass of fragments |
| $r$ | crack dimension, or fragment dimension |
| $r_{\min}$ | minimum crack advancement, or minimum fragments size |
| $r_{\max}$ | maximum fragment size |
| $T$ | period of the oscillation |
| $V$ | concrete specimen volume |
| $x_0$ | initial value of an AE signal oscillation |
| $x_{\min}$ | minimum detectable value of an AE signal oscillation |
| $\Delta t$ | time interval |
| $\delta$ | damping |
| $\delta_{\text{cr}}$ | critical damping |
| $\varepsilon$ | strain |
| $\zeta = \delta/\delta_{\text{cr}}$ | relative damping |
| $\lambda_{\text{n}}$ | circular frequency |
| $\sigma$ | stress |

* Department of Structural Engineering and Geotechnics, Politecnico di Torino, Corso Duca degli Abruzzi 24, 10129 Torino, Italy.

## Introduction

One of the most successful applications of acoustic emissions (AE) consists of detecting the presence of discontinuities or cracks, and their location, in concrete

specimens and structures. The AE technique has been used in load testing of concrete structures and specimens. It is a passive non-destructive technique, and acoustic signals are emitted only when a permanent, non-reversible deformation occurs inside a material. The AE technique is extremely useful for detecting the formation of cracks and microcracks in concrete structures.[1–9]

The AE monitoring technique is similar to the one employed in earthquake control, where seismic waves reach the monitoring stations situated on the surface of the earth. As a rule, acoustic emissions are acquired by means of piezoelectric transducers (PZT) that exploit the property of certain crystals to generate electrical signals whenever they are subjected to mechanical stresses. Transducers can be resonant or wide band, and must be calibrated on frequency values of between 50 and 800 kHz. The acquisition of the ultrasonic signals owing to cracking, especially *p*-waves, is by means of transducers connected to control units that are able to process the signals received.[6,8] Although they take place on very different scales, these two families of phenomena— damage in structural materials and earthquakes in geophysics—are very similar: in either case, in fact, there is a release of elastic energy from sources located inside a medium. Another similarity between complex seismic phenomena and damage processes in structures, as assessed by means of the AE technique, is provided by the statistical distribution of earthquakes: high magnitude earthquakes, in fact, are less frequent than lighter quakes, this phenomenon is quantified by the first Gutenberg–Richter (GR) law.[10] The validity of this analogy has been confirmed by various authors, who demonstrated how the amplitude of the AE signals, associated with the formation of microcracks in the structural elements monitored, follows the GR power law frequency–magnitude statistics.[5,8,11] They also measured the cumulative energy in the acoustic emission activity and found that this activation is very similar to the power law seismic activation in the geological faults, as demonstrated by the second GR law.[10,11]

A very important aspect of this is that, in many kinds of structures, especially very complex or highly redundant ones, there are places where stresses are low, or even approach zero. These low stress areas do not emit, and therefore will not interfere with AE monitoring results; however, this does not rule out the possibility that stresses in other areas can be high enough to undermine the bearing capacity of a construction. In this manner, once the damaged or cracked parts of a structure, which generally correspond to the zones where stresses are highest, have been identified, the AE method makes it possible to assess the evolution of damage and predict whether it will gradually come to a halt or will propagate faster and faster. With this criterion, by distributing several sensors covering adjacent areas, it proves possible to take into account stress redistribution capacities even in a complex structure.

This method was applied by the current authors to the monitoring of reinforced concrete structures and masonry structures by arranging the sensors in the zones subject primarily to high compressive stresses.[1–7] Moreover, based on fractal concepts, a multiscale criterion has been formulated to predict the propagation of damage in concrete structural elements. According to this method, the damage level of a structure can be estimated from AE data obtained on a reference specimen extracted from a structure and tested up to failure.[1,6]

The aim of the present study is to demonstrate how the GR laws do not amount to a simple experimental observation also based on the AE monitoring process, but rather constitute a theoretical interpretation of the AE activity. Based on these considerations, the energy density dissipated during compression and fragmentation of heterogeneous quasi-brittle materials was evaluated. This innovative method is substantially based on the acoustic emission technique and on fractal geometry. The results obtained from a great number of tests performed on specimens drilled from a real structure were used to evaluate scale effects on AE activity.[1,2,6] A statistical and fractal analysis has been also performed to take into account the multiscale aspect of cracking phenomena. This approach made it possible to verify the two semi-empirical GR laws,[10] widely used in seismology, whose fractal interpretation is very close to the essence of the AE phenomenon.[11,12] The fractal theory, based on the geometrical self-similarity of structural defects, has the aim of defining simple but rigorous laws, useful to evaluate the energy progressively released by a compressed structural element.

By applying these criteria to AE analysis it is possible to obtain a better understanding of the relationship between microstructural events and macroscopic behaviour and reach a better position to formulate predictive models, either about laboratory scale effects or full-size structural performance and reliability. In this manner, the methods used for the study of earthquakes and other seismic phenomena can be transferred to materials sciences and can provide useful criteria for the control of civil structures.

## Fundamentals of AE technique

Cracking is accompanied by emission of elastic waves, which propagate within bulk material. These waves can be received and recorded by transducers applied on the surface of the structural element.[8] The AE method, which is called ring-down counting or event-counting, considers the number of waves beyond a certain threshold level and is widely used for defect analysis.[9,13] As a first approximation, in fact, the cumulative number of counts $N_c$ can be compared with the amount of energy released during the loading process, assuming that both quantities increase with the extent of damage (Fig. 1). The quantity that characterises the distribution of peak amplitude is the cumulative distri-

bution $N(v)$, which represents the number of recorded signals with peak amplitude larger than $v$ (measured in volts). Similar analyses are commonly carried out, at different scales, in seismology, where it was demonstrated that a larger number of emissions corresponds to smaller amplitudes, whereas larger amplitudes are restricted to fewer events.[10,11,14]

## Experimental set-up

### Test specimens and testing equipment

As pointed out in the Introduction, all the cylindrical specimens were obtained by drilling from a real concrete structure.[1,2,6] The concrete, of poor mechanical characteristics, has an apparent specific weight of about $2·23$ g/cm$^3$ and a maximum aggregate size of about 15 mm. The cement amount is around 100 kg/m$^3$. Three different diameters are considered in a maximum scale range of 1:3·6. The specimens present a height/diameter ratio $h/d = 1$ and $d$ is chosen equal to 27·5, 59, 99 mm, respectively. Six identical specimens have been tested for $d = 99$ and 59 mm, and three identical specimens for $d = 27·5$ mm. The tests have been performed by an electronic controlled Servo-hydraulic Material Testing Systems machine (810 model) with a capacity of 250 kN.[1,2,6] This kind of machine is controlled by an electronic closed-loop servo-hydraulic system. It is therefore possible to perform tests under load or displacement control. The displacements are recorded by a couple of inductive-bridge transducers (Hottinger Baldwin Measurements Inc. W10 model) applied on the loading platens, with a maximum stroke of 10 mm (Fig. 2). The geometries of the tested specimens and the average values obtained from the experiments are summarised in Table 1.

### Displacement control and boundary conditions

The system adopted in the compression test utilises rigid steel platens. All compression tests have been performed under displacement control, by imposing a constant rate of the displacement of the upper loading platen. A displacement rate equal to $4 \times 10^{-4}$ mm/s was adopted for all specimens, in order to obtain a very slow crack growth and to detect all possible AE signals. In this way, it was possible to also capture the softening branch of the stress–strain diagrams (Fig. 3).

### AE data acquisition system

The apparatus consists of two PZTs, applied on the specimen surface and calibrated in the frequency range between 50 and 500 kHz, and of two data acquisition systems.[1,2,6] The threshold level of the signal is set equal to 100 $\mu$V and it is amplified up to 100 mV. According to the literature, this represents the typical value used for AE measurements in concrete.[8,15] The oscillation counting capacity has been set equal to 255 counts in 120 s, that is, a single event is the result of 2 recording minutes. By means of this system, the intensity of a single event is calculated assuming that the amplitude $v$ of the signals is proportional to the number of counts $N$ recorded in the time interval (event-counting). Clearly, this hypothesis is fully justified in the presence of slow crack growth.
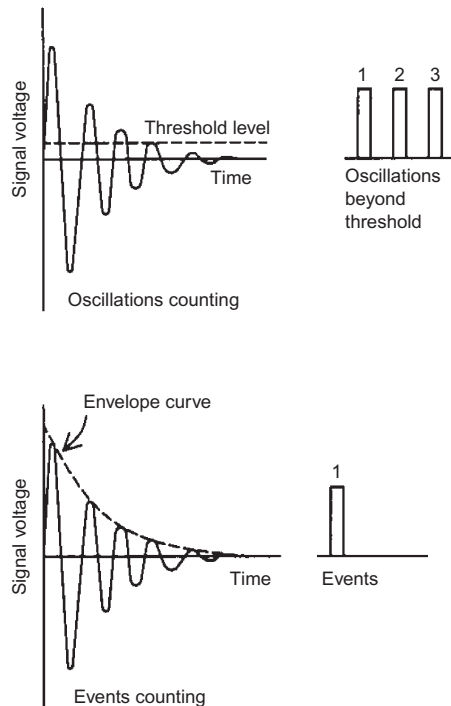
## Typical AE activity under compression

The global scale-dependent behaviour of concrete in compression can be explained by linear elastic fracture mechanics (LEFM), which contemplates energy dissipation over fracture surfaces.[16,17] Moreover, the stress against time curve for a specimen of medium size, characterising the AE activity, is represented in Fig. 3. Compressive stress, cumulated event number $N_c$ and event rate (per each couple of minutes) are depicted in Fig. 3(a).

Figure 3(b) shows compressive stress and cumulated event number as functions of nominal strain. In the same diagram, the derivative of the cumulative curve is also reported. The AE data in Fig. 3(b) are divided into six regimes according to the stress level (loading stages), from (a) to (f), for the convenience of analysis. The compressive stress is calculated from the imposed compressive load divided by the original cross-sectional area. The nominal strain is the elongation, measured by the control inductive bridge transducer, and divided by the original height of the specimen. In regime (a), which is the initial portion of the stress–strain curve, few AE events can be recorded because the stress level is rather
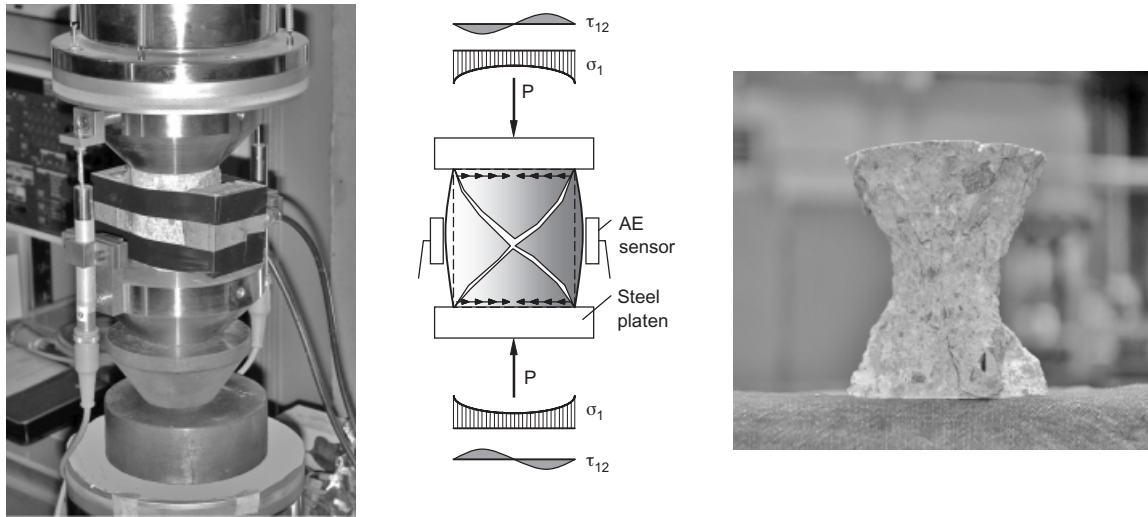


*Fig. 1. Detected signals by AE technique*

*Fig. 2. Compression tests and typical shear failure of a concrete specimen*

Table 1. *Average values obtained from experiments*

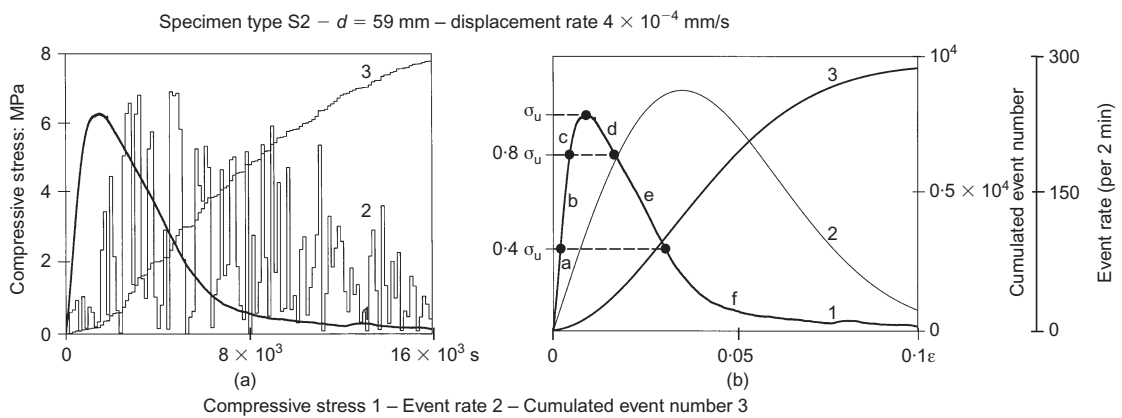| Specimen type | Diameter: mm | Peak load: daN | Stress at peak load $\sigma_u$: MPa | Stress–strain area up to $\varepsilon = 0.05$; MPa | $N_C$ number at $\varepsilon = 0.05$ | $N_C$/Vol. at $\varepsilon = 0.05$ |
|---|---|---|---|---|---|---|
| S1 | 27·5 | 451·4 | 7·6 | 0·216 | 2500 | 0·153 |
| S2 | 59 | 1941·2 | 7·1 | 0·181 | 7000 | 0·043 |
| S3 | 99 | 5003·5 | 6·5 | 0·167 | 9500 | 0·012 |



*Fig. 3. Compressive stress and AE signals as functions of time or strain*

low at this loading stage. After that, a sensible AE activity starts to be detectable around 42–45% of the peak stress ($\sigma_u$), in regime (b), where the stress level is within the interval 0·4–0·8 $\sigma_u$. In this regime, a small but gradually increasing number of AE events can be recorded, although the material is still deformed elastically. Such a gradually increasing amount of AE events extends to regime (c), in which the stress level varies from 0·8 $\sigma_u$ to $\sigma_u$ and the stress–strain response is non-linear. The event rate reaches its maximum value at the beginning of regime (f), in the softening branch of the diagram, where the compressive stress is around 0·4 $\sigma_u$.

This remark implies that the AE activity is closely related to this loading stage, where the central portion of the specimen undergoes extensive cracking that dominates the emission.

## AE activity interpreted by GR laws

The GR laws are substantially empirical.[10,11,14] In this section their theoretical interpretation based on the fractal approach is suggested.

The first GR law can be written as

$$\log n = C - bm \tag{1}$$

where $n$ is the number of events with intensity larger than $m$, and $C$ and $b$ are experimental constants. On the other hand, the second law reads

$$\log E = \bar{C} + am \tag{2}$$

where $E$ represents the energy released by a single event of intensity $m$, and $\bar{C}$ and $a$ are experimental constants. Inserting equation (2) into equation (1) gives the following relationship

$$\log n = \bar{\bar{C}} - c \log E \tag{3}$$

The last equation can be directly obtained assuming a fractal (self-similar) distribution in the size of the cracks:[18,19]

$$n/n_{\text{tot}} = (r_{\min}/r)^D \tag{4}$$

The above distribution simply means that there is a power-law correlation between the number of events $n$ (crack propagation) with advancement (of the crack) larger than $r$, and $r$ itself. In equation (4), $D$ is the so-called fractal exponent, $r_{\min}$ is the minimum crack advancement and $n_{\text{tot}}$ is the total number of events.

The fractal hypothesis of equation (4) describes a self-similar process that is typically verified from an experimental point of view.[12] A similar equation has been recently proposed for comminution processes,[18,19] in which $n$ represents the number of particles with radius larger than $r$ obtained from fragmentation. It represents the cumulative distribution function for the fragment size probability density, that can be integrated to compute the mass of particles with radius smaller than $r$

$$M(< r) \propto \int_{r_{\min}}^{r} r^3 \mathrm{d}n \propto \left( r^{3-D} - r_{\min}^{3-D} \right) \cong r^{3-D} \tag{5}$$

The last equality is valid for the usual values of $D$ lower than 3, so that the ratio of this partial mass to the total mass of fragments becomes

$$M(< r)/M \cong (r/r_{\max})^{3-D} \tag{6}$$

It is very interesting to note that each type of energy involved in the process, for example, to create fracture surfaces (dissipated), as well as transformed into kinetic energy (released), can be assumed as proportional to the surface area of the crack,[18,19] that is, $E \propto r^2$. Even if it is quite intuitive for fracture energy (according to the Griffith assumption) it is true also for the kinetic energy released in the AE process.

According to these considerations and assuming $E \propto r^2$, equation (4) becomes

$$n/n_{\text{tot}} = (E_{\min}/E)^{D/2} \tag{7}$$

or

$$\log \frac{n}{n_{\text{tot}}} = -\frac{D}{2} \log \frac{E}{E_{\min}} \tag{8}$$

that is coincident with equation (3), with $c. \cong D/2$

A dynamic system is now considered with given properties of inertia, stiffness and damping. Attention is focused on a single degree of freedom system with mass $\bar{m}$, stiffness $k$ and damping $\delta$. After an event (impulse), the displacement of the structure will correspond to a damped oscillation with amplitude from an initial value $x_0$ to a final value $x_{\min}$.[20] The existence of a minimum non-zero value for the displacement is connected with the experimental apparatus sensitivity. $N$ is the number of oscillations, occurring in a time $\Delta t$, between these two extreme values. The ratio between initial and minimum displacements can be easily obtained as

$$x_0/x_{\min} = e^{\zeta \lambda_n \Delta t} \tag{9}$$

with $\lambda_n = \sqrt{k/\bar{m}}$ and $\zeta = \delta/\delta_{\text{cr}}$, where $\delta_{\text{cr}} = 2\sqrt{k\bar{m}}$ is the critical damping of the structure. The energy $E$ of the considered event will be proportional to $x_0^2$, as well as the interval $\Delta t$ will be equal to $NT$, $T = 2\pi/(\lambda_n \sqrt{1 - \zeta^2})$ being the (pseudo-) period of the oscillation. As a consequence, the energy becomes

$$E/E_{\min} = e^{2\zeta \lambda_n NT} \tag{10}$$

or, in an equivalent form[20]

$$\log \frac{E}{E_{\min}} = \frac{4\pi\zeta}{\sqrt{1 - \zeta^2}} N \tag{11}$$

that is coincident with equation (2), if the number of oscillations $N$ (which does not fit with the number $n$ of events previously introduced) is proportional to the magnitude $m$ of the event in particular it is expected (for $E \cong E_{\min}$, $m = 0$):

$$m = \log \frac{E}{E_{\min}} = \frac{4\pi\zeta}{\sqrt{1 + \zeta^2}} N \tag{12}$$

Equation (12) shows that in the GR laws the magnitude of an event can be considered proportional to the number of oscillations owing to the event and that $a \cong 1$. In addition, the equivalence between equations (3) and (8) as well as between equations (2) and (11) represents the theoretical interpretation of the two GR laws.

*Acoustic emission during compression*

During a compression test the amount of energy dissipated typically by crack propagation can be detected step by step by acoustic emission.

In particular, from equation (8) and taking into account equation (11) the following is obtained

$$\log \frac{n}{n_{\text{tot}}} = -\frac{2\pi D\zeta}{\sqrt{1 - \zeta^2}} N \tag{13}$$

that is coincident with equation (1) with $b \cong D/2$, or

$$E(N)/E_{\min} = e^{(4\pi\zeta/\sqrt{1-\zeta^2})N} \qquad (14)$$

The constant of proportionality $E_{\min}$ is unknown and can be determined imposing that at the end of the compression test the energy dissipation is coincident with the volume $V$ of the specimen times the area under the stress–strain curve, that is, with the total energy dissipated

$$E_{\min} = \frac{V\int\sigma\,d\varepsilon}{\sum_{i=1}^{I_{\text{TOT}}} e^{(4\pi\zeta/\sqrt{1-\zeta^2})N_i}} \qquad (15)$$

$I_{\text{TOT}}$ being the total number of steps. The energy dissipation at a generic step $I$ during the compression test can be predicted as

$$E(I) = E_{\min}\sum_{i=1}^{I} e^{(4\pi\zeta/\sqrt{1-\zeta^2})N_i} \qquad (16)$$

*Experimental assessment*

A comparison between experimental results and theoretical predictions is herein presented. The example regards a specimen type S1, with $d$ equal to 27·5 mm. Submitting the fragments of this specimen to a statistical analysis, the parameter $D$ is quantified in equation (6). This parameter represents the slope, in the bilogarithmic plane, of the diagram that relates mass and relative fragment size. From the best fit, the slope $3 - D \cong 0·75$ is obtained, Fig. 4(a), so that the fractal exponent is $D \cong 2·25$. Note that such fractal exponent can be estimated according to three independent methodologies, namely size effects on dissipated energy density,[19] particle size distribution[19] and acoustic emission scaling.[3] The stress plotted against time curve, with cumulated event number, is represented in Fig. 4(b), while the distribution of events $n/n_{\text{tot}}$ versus $N$ (number of oscillations per each couple of minutes) during the compression test, is reported in Fig. 4(c). Comparing the best-fit straight line, obtained from the experimental results, with equation (13), the $\zeta$ para-
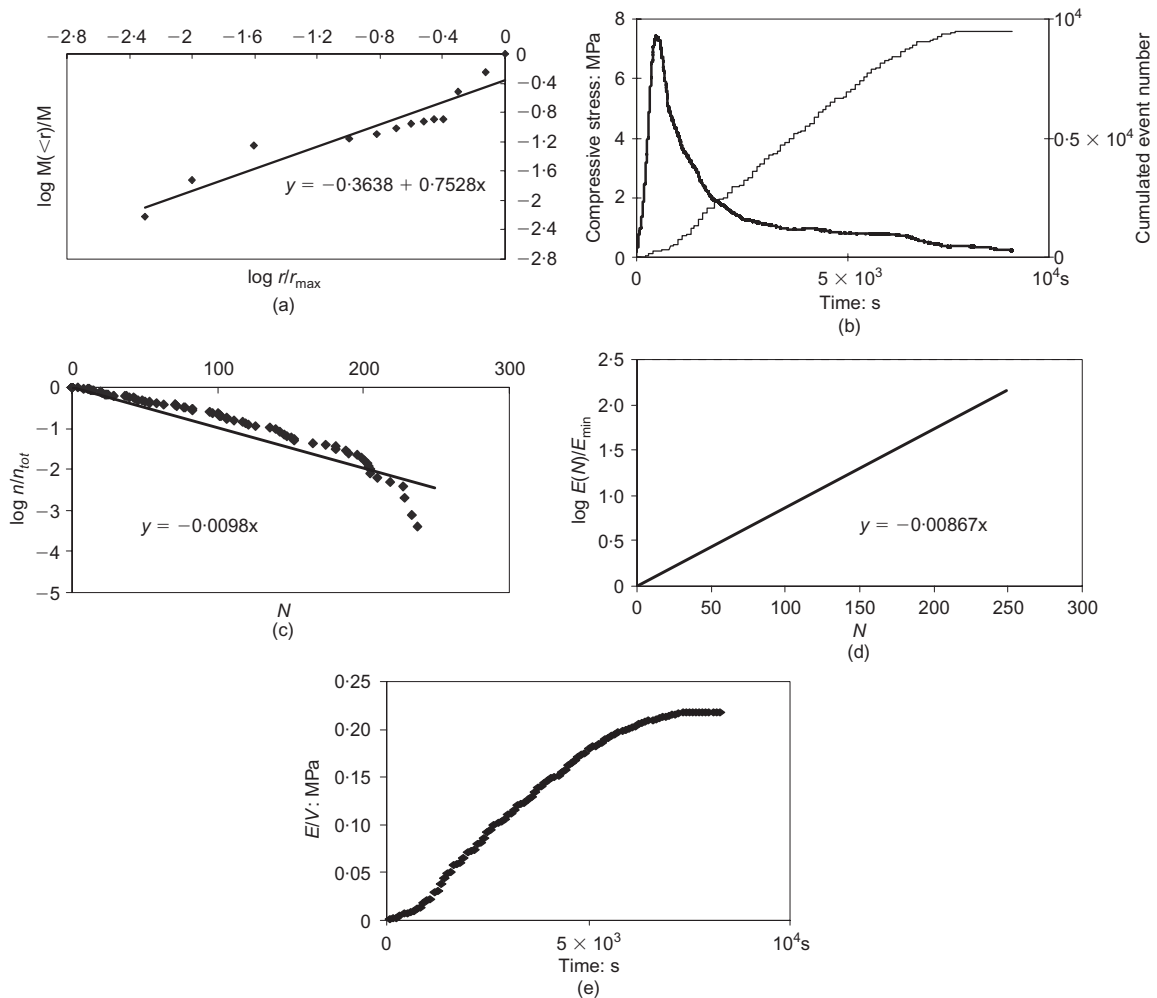


Fig. 4. Diagrams referring to the experimental assessment

meter is $6.9 \times 10^{-4}$. At this point it is possible to represent from equation (14) the theoretical energy dissipation as a function of the number of oscillations (Fig. 4(d)). Calculating the area under the stress–strain curve of Fig. 4(b), the value $E_{\min}$ is obtained from equation (15). Finally, the energy dissipation at a generic step, during the compression test, is obtained by equation (16) (Fig. 4(e)).

## Conclusions

The aim of the present study is to demonstrate how the GR laws, on which seismology is based, do not amount to a simple experimental observation which also depends on the AE monitoring process, but rather constitute a theoretical interpretation of the acoustic emission activity.

For the interpretation of the two well-known empirical GR laws, the acoustic emission technique and fractal geometry were relied upon. Furthermore, this approach made it possible to identify the 'magnitude' parameter, appearing in the laws, with the number of oscillations larger than a given threshold (the sensitivity of the experimental apparatus to measure the acoustic emission after a given event). Finally, these concepts were applied to the study of the compression phenomena. In particular, with this approach, it is now possible to distinguish between the energy progressively dissipated or stored in a compressed structural element.

In this manner, the methods used for the study of earthquakes and other seismic phenomena can be transferred to the science of materials and can provide useful criteria for the control of civil structures. By applying these criteria to AE analysis, a better understanding is gained of the relationship between microstructural events and macroscopic behaviour and it becomes more probable that predictive models can be formulated, either about laboratory scale effects or full-size structural performance and reliability.

## Acknowledgements

## References

1. CARPINTERI A., LACIDOGNA G. and PUGNO N. Damage diagnosis and life-time assessment of concrete and masonry structures by an acoustic emission technique. In *Proceedings of 5th International Conference on Fracture Mechanics of Concrete and Concrete Structures* (*FraMCos-5*), Vail, Colorado, USA (LI V. C., LEUNG C. K. Y., WILLAM K. J. and BILLINGTON S.L. (eds)). International Association for Fracture Mechanics of Concrete and Concrete Structures, Evanston, IL, USA, 2004, Vol. 1, pp. 31–40.

2. CARPINTERI A. and LACIDOGNA G. Structural monitoring and diagnostics by the acoustic emission technique: scaling of dissipated energy in compression. *Proceedings of the 9th International Congress on Sound and Vibration* (*ICSV9*), Orlando, Florida, 2002, CD-ROM, paper 166.

3. CARPINTERI A., LACIDOGNA G. and PUGNO N. A fractal approach for damage detection in concrete and masonry structures by the acoustic emission technique. *Acoustique et Techniques*, 2004, **38**, No. 3, 31–37.

4. CARPINTERI A., LACIDOGNA G. and PUGNO N. Time scale effects on acoustic emission due to elastic waves propagation in monitored cracking structures. *Physical Mesomechanics*, 2005, **8**, No. 5–6, 77–80.

5. CARPINTERI A., LACIDOGNA G. and NICCOLINI G. Critical behaviour in concrete structures and damage localization by acoustic emission. *Key Engineering Materials*, 2006, **312**, 305–310.

6. CARPINTERI A., LACIDOGNA G. and PUGNO N. Structural damage diagnosis and life-time assessment by acoustic emission monitoring. *Engineering Fracture Mechanics*, 2006, in press, doi: 10.1016/j.engframech.2006.01.036.

7. CARPINTERI A. and LACIDOGNA G. Structural monitoring and integrity assessment of medieval towers. *ASCE Journal of Structural Engineering*, 2006, accepted for publication.

8. OHTSU M. The history and development of acoustic emission in concrete engineering. *Magazine of Concrete Research*, 1996, **48**, No. 177, 321–330.

9. POLLOCK A. A. Acoustic emission-2: acoustic emission amplitudes. *Non-Destructive Testing*, 1973, **6**, No. 5, 264–269.

10. RICHTER C. F. *Elementary Seismology*. W. H. Freeman, San Francisco and London, 1958.

11. RUNDLE J. B., TURCOTTE D. L., SHCHERBAKOV R., KLEIN W. and SAMMIS C. Statistical physics approach to understanding the multiscale dynamics of earthquake fault systems. *Reviews of Geophysics*, 2003, **41**, No. 4, 1–30.

12. PETRI A., PAPARO G., VESPIGNANI A., ALIPPI A. and COSTANTINI M. Experimental evidence for critical dynamics in microfracturing processes. *Physical Review Letters*, 1994, **73**, No. 25, 3423–3426.

13. BRINDLEY B. J., HOLT J. and PALMER I. G. Acoustic emission-3: the use of ring-down counting. *Non Destructive Testing*, 1973, **6**, No. 5, 299–306.

14. CHAKRABARTI B. K. and BENGUIGUI L. G. *Statistical Physics of Fracture and Breakdown in Disordered Systems*. Clarendon Press, Oxford, 1997.

15. SHAH P. and LI Z. Localization of microcracking in concrete under uniaxial tension. *ACI Materials Journal*, 1994, **91**, No. 4, 372–381.

16. CARPINTERI A., FERRO G. and MONETTO I. Scale effects in uniaxially compressed concrete specimens. *Magazine of Concrete Research*, 1999, **51**, No. 3, 217–225.

17. CARPINTERI A., CIOLA F. and PUGNO N. Boundary element method for the strain-softening response of quasi-brittle materials in compression. *Computers and Structures*, 2001, **79**, No. 4, 389–401.

18. CARPINTERI A. and PUGNO N. One, two, and three-dimensional universal laws for fragmentation due to impact and explosion. *Journal of Applied Mechanics*, 2002, **69**, No. 6, 854–856.

19. CARPINTERI A., LACIDOGNA G. and PUGNO N. Scaling of energy dissipation in crushing and fragmentation: a fractal and statistical analysis based on particle size distribution. *International Journal of Fracture*, 2004, **129**, No. 2, 131–139.

20. TETELMAN A. S. and EVANS A. G. Failure prediction in brittle materials using fracture mechanics and acoustic emission. *Proceedings of the Symposium on Fracture mechanics of ceramics*, 1974, pp. 895–924.

**Discussion contributions on this paper should reach the editor by 1 May 2007**